Electro/Ni Dual-Catalyzed Decarboxylative C(sp^3)−C(sp^2) Cross-Coupling Reactions of Carboxylates and Aryl Bromide

Jian Luo,[a] Michael T. Davenport,[b] Daniel H. Ess,[*b] and T. Leo Liu[*a]

a. Department of Chemistry and Biochemistry, Utah State University, Logan, Utah 84322, United States

b. Department of Chemistry and Biochemistry, Brigham Young University, Provo, Utah 84604, United States

Corresponding: dhe@chem.byu.edu, leo.liu@usu.edu

Abstract: Paired redox-neutral electrolysis offers an attractive green platform for organic synthesis by avoiding sacrificial oxidants and reductants. Here, we report the electro/Ni dual-catalyzed redox-neutral C(sp^3)−C(sp^2) cross-coupling reactions between carboxylates and aryl bromides. At a cathode, an Ni^{II}(Ar)(Br) intermediate is formed through the activation of the Ar−Br bond by a Ni^{I}-bipyridine catalyst and subsequent one electron reduction. The carboxylates, including amino acid, benzyl carboxylic acid, and 2-phenoxy propionic acid, undergo oxidative decarboxylation at an anode to form carbon based radicals. The combination of the Ni^{II}(Ar)(Br) intermediate and the carbon radical results in the formation of C(sp^3)−C(sp^2) cross-coupling products. The broad reaction scope, excellent functional group tolerance, and good yields of the electro/Ni dual-catalyzed C(sp^3)−C(sp^2) cross-coupling reaction were confirmed through 48 examples of carboxylates and aryl bromides in small-scale vial reactions and scale-up flow synthesis. The electro/Ni dual-catalyzed cross-coupling reactions described in this study are expected to have broad applications in the construction of C(sp^3)−C(sp^2) bonds because of the readily available carboxylate nucleophiles and the scalability of electrochemical flow-synthesis technology.

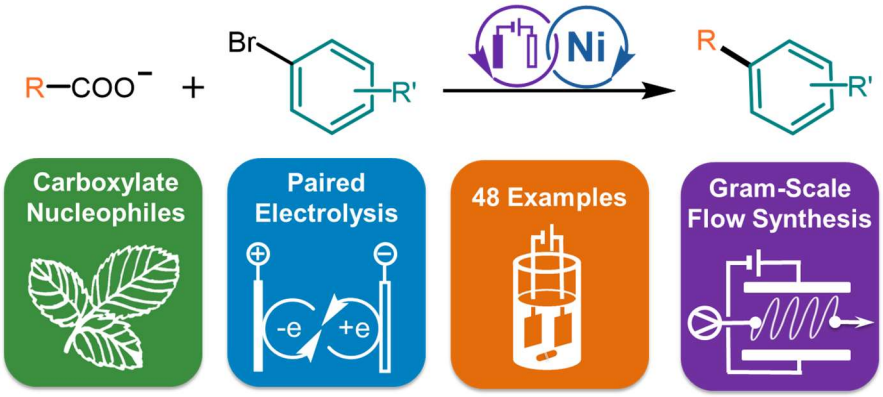

Introduction

Nickel-catalyzed C−C cross-coupling reactions have expanded the field of synthetic chemistry and enabled new methods for constructing molecular skeletons.[1-4] In recent years, a variety of Ni-catalyzed C−C cross-coupling reactions, such as Kumada–Corriu, Suzuki–Miyaura, Negishi, Mizoroki–Heck, and reductive cross-electrophile coupling reactions, have been developed and applied in the synthesis of pharmaceuticals and natural products.[5-8] Despite the significant success of Ni-catalyzed C−C cross-coupling reactions, these methodologies still suffer from several well-known limitations, including the use of highly active nucleophiles (such as Grignard reagents and organozinc reagents), sacrificial reductants, sensitive precatalysts (such as bis(cyclooctadiene)nickel(0)), and sometimes elevated reaction temperatures.[1,2,6,9] There remains significant interest in developing Ni-catalyzed C−C cross-coupling reactions with mild conditions, using readily available and affordable substrates, and bench-stable reagents and catalysts.

Directly employing electrodes as both the oxidant and reductant, paired redox-neutral electrolysis offers an attractive platform for C−C cross-coupling reactions because it avoids the need for stoichiometric amounts of sacrificial oxidants and reductants.[10-13] In paired electrolysis, highly reactive intermediates such as catalyst intermediates and carbon radicals are formed *in situ* through electrochemical reactions. No strong reagents or sensitive precatalysts are required in the reactions.[10,11] Previously, Hu *et al.* and our group independently reported anodic oxidation of nucleophiles and cathodic reduction of organic halides to enable efficient Ni-catalyzed redox-neutral $C(sp^3)$–$C(sp^2)$ cross-coupling reactions between toluene derivatives or benzyl trifluoroborate and organic halides, respectively (Scheme 1C).[14,15] However, the limited flexibility of the toluene derivative substrates and inconvenient synthesis of trifluroborate nucleophiles

restricts the widespread application of these methodologies. Therefore, a major goal of our recent studies was to significantly expand the range of nucleophiles in the redox neutral C(sp^3)–C(sp^2) cross-coupling reactions.

Scheme 1. Kolbe-type Reactions and Electrochemical Redox-Neutral C(sp^3)–C(sp^2) Cross-Coupling Reactions.

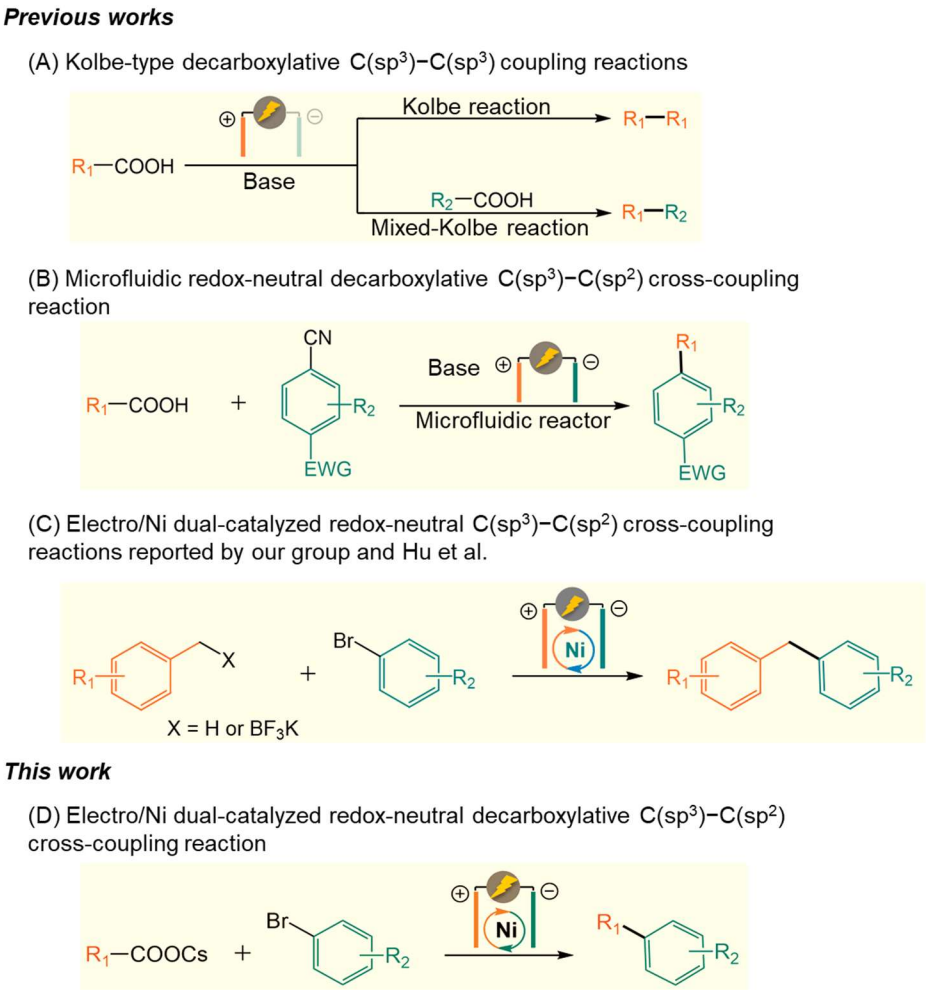

Carboxylates are non-toxic, stable, inexpensive, and widely available and have been extensively utilized as nucleophiles in transition-metal catalyzed C–C cross-coupling reactions.[16-18] Under electrochemical conditions, carboxylates undergo decarboxylative radicalization through single-electron transfer oxidation at the anode.[19,20] Several valuable reactions have been developed by using this type of electrogenerated carbon radical.[10,18-20] For example, the Kolbe-type decarboxylative C(sp^3)–C(sp^3) radical coupling reactions have been known for 170 years (Scheme 1A).[21] Several mixed-Kolbe reactions using a combination of two different carboxylates to achieve

$C(sp^3)$–$C(sp^3)$ cross-coupling have also been developed.[10] Recently, Baran and coworkers overcame the limitations of Kolbe coupling by using waveform-controlled electrosynthesis and achieved good selectivity for $C(sp^3)$–$C(sp^3)$ cross-coupling.[22] However, due to the local high concentration of reactive carbon radicals in the double layer of the anode during electrolysis, it is extremely challenging to effectively combine the carbon radicals generated from anodic decarboxylation with the intermediates generated from cathodic reduction to achieve redox-neutral $C(sp^3)$–$C(sp^2)$ cross-coupling. There is one reported example of a redox-neutral electrochemical decarboxylative $C(sp^3)$–$C(sp^2)$ cross-coupling reaction realized in a microfluidic reactor (Scheme 1B).[23] In this reaction, anodic decarboxylation produces a carbon radical, which is then trapped by a long-lifetime electron-deficient aryl nitrile radical anion generated from cathodic reduction. After the departure of the cyanide anion, a $C(sp^3)$–$C(sp^2)$ cross-coupling product is produced.

Electro/Ni dual-catalyzed reductive decarboxylative $C(sp^3)$–$C(sp^2)$ cross-coupling reactions between aryl or alkenyl halides and redox-active N-hydroxyphthalimide (NHP) esters derived from alkyl carboxylic acids have been reported.[24,25] In these reactions, a Mg anode is required to balance the charge, and an $AgNO_3$ additive is used to modify the cathode *in situ*. In contrast, the electro/Ni dual-catalyzed redox-neutral decarboxylative $C(sp^3)$–$C(sp^2)$ cross-coupling reactions that avoid the use of sacrificial anodes have not been developed. In this work, we report the electro/Ni dual-catalyzed redox-neutral decarboxylative $C(sp^3)$–$C(sp^2)$ cross-coupling reactions between carboxylates and aryl bromides (Scheme 1D). Amino acid, benzyl carboxylic acid, and 2-phenoxy propionic acid carboxylates undergo oxidative decarboxylation at the anode to form carbon-centered free radicals. The combination of the carbon radical and an $Ni^{II}(Ar)(Br)$ intermediate formed through cathodic reduction results in the formation of $C(sp^3)$–$C(sp^2)$ cross-coupling products. High reaction efficiency and potential applications of this cross-coupling reaction were demonstrated through 48 examples of carboxylates/aryl bromides and gram-scale flow synthesis. The reaction mechanism was systematically studied through electrochemical voltammetry and density functional theory (DFT) calculations. The electro/Ni dual-catalyzed cross-coupling reactions described in this work are expected to have broad applications in the construction of $C(sp^3)$–$C(sp^2)$ bonds because of readily available carboxylate nucleophiles and the scalability of the electrochemical flow-synthesis technology.

Results and Discussion

We envisioned that the ability of carboxylates to serve as carbon radical precursors for electro/Ni dual-catalyzed decarboxylative $C(sp^3)$–$C(sp^2)$ cross-coupling could be determined by the electrochemical activity of the carboxylates and the stability of the generated carbon radicals. Therefore, we first performed cyclic voltammetry (CV) scanning to detect the electrochemical activity of a library of carboxylates, including terminal alkyl carboxylate (cesium 3-phenylpropionate (**1**)), benzyl carboxylate (cesium phenylacetate (**2**)), α-heteroatom substituted carboxylate (N-benzoyl-DL-alanine cesium salt (**3**) and cesium tetrahydrofuran-2-carboxylate (**4**)), quaternary carboxylate (cesium 1-methyl-1-cyclohexanecarboxylate (**5**)), and aryl carboxylate (cesium benzoate (**6**)). As shown in Figure 1A, compounds **3** and **4** exhibited the lowest onset oxidation potential at +0.24 V (vs. $Fc^{+/0}$). This indicates that compounds **3** and **4** are thermodynamically most easy to oxidize. Compounds **1**, **2**, and **5** exhibited medium onset oxidation potentials at +0.48 V, +0.44 V, and +0.40 V (vs. $Fc^{+/0}$), respectively. Due to the electron-withdrawing effect of the aryl group, compound **6** exhibited the highest onset oxidation potential at +0.76 V (vs. $Fc^{+/0}$). In addition, compound **3** delivered the highest peak current density, indicating that a high electrochemical rate at the surface of the glassy carbon working electrode.[26] According to these results, compound **3** is the most electrochemically active carboxylate among compounds **1**-**6**. We also tested sodium and potassium carboxylates. They showed similar electrochemical behaviors as the cesium salts in the CV measurements. However, they are not good substrates in electrochemical synthesis because of their poor solubility in DMF.

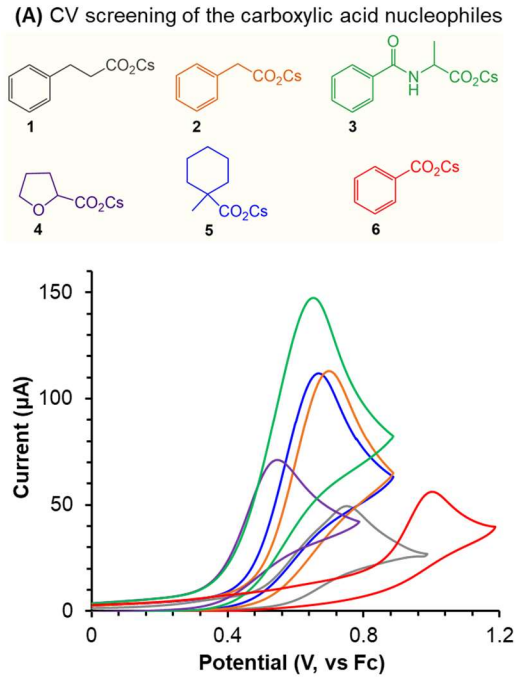

(B) Optimization for the electro/Ni dual-catalyzed redox-neutral decarboxylative C(cs^3)−C(sp^2) cross-coupling reaction

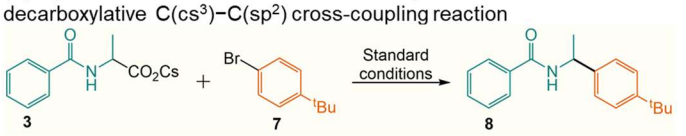

Entry	Variation from standard conditions	Yield of **8** (%)
1	None	72
2	No dtbbpy ligand	0
3	No $NiBr_2$.glyme	0
4	No current	0
5	No $LiClO_4$	0
6	$TBAPF_6$instead of $LiClO_4$	52
7	KPF_6 instead of $LiClO_4$	67
8	2,2'-bpy instead of dtbbpy	27
9	1,10-phen instead of dtbbpy	64
10	tpy instead of dtbbpy	66 (64 h)
11	2.5 mA current electrolysis	70 (72 h)
12	10 mA current electrolysis	13

Figure 1. Electrochemical scanning of carboxylate nucleophiles and reaction optimization. (A) CV screening of the carboxylate nucleophiles; (B) Optimization for the electro/Ni dual-catalyzed redox-netral decarboxylative C(sp^3)−C(sp^2) cross-coupling reaction of **3** and **7**. Standard conditions: 211 mg (0.65 mmol) **3**, 107 mg (0.5 mmol) **7**, 20 mg (0.75 mmol) dtbbpy, 16 mg (0.05 mmol) $NiBr_2$·DME, 0.2 M $LiClO_4$, 6 mL dry DMF, RVC (+/-), 5 mA current for 30 h.

With knowledge of the electrochemical activities of several carboxylates, we investigated the electro/Ni dual-catalyzed decarboxylative C(sp^3)−C(sp^2) cross-coupling reaction using compound **3** as the carbon radical precursor. In an initial trial, a combination of nucleophile **3**, aryl bromide electrophile **7**, $NiCl_2$·DME pre-catalyst, 2,2'-bpy ligand, and $LiClO_4$ supporting electrolyte in DMF was used. After galvanostatic electrolysis at 5.0 mA for 30 hours, a 27% yield of the decarboxylative C(sp^3)−C(sp^2) cross-coupling product **8** was obtained (entry 8 in Figure 1B). N-vinylbenzamide is a side product with a 41% yield (Figure S1). To further optimize the reaction, various ligands (1,10-phen, tpy, and dtbbpy), supporting electrolytes ($TBAPF_6$ and KPF_6), and solvents were screened. The highest yield of product **8**, 72%, was achieved by using the combination of the dtbbpy ligand, $LiClO_4$ supporting electrolyte, and dry DMF solvent. The choice of supporting electrolyte had a moderate impact on the reaction efficiency. When $TBAPF_6$ and KPF_6 were used instead of $LiClO_4$, the yields of product **8** decreased to 52% and 67%, respectively (entries 6 and 7 in Figure 1B). 1,10-Phen and tpy ligands gave slightly lower yields of 64% and

66%, respectively (entries 9 and 10 in Figure 1B). Additionally, in the presence of tpy ligand, the reaction was significantly slowed down, taking 64 hours to complete. Switching to other solvents, only DMSO yielded 43% of product **8** (Table S1). THF, MeCN, CH_2Cl_2, and MeOH were ineffective for the reaction as **8** was not produced. It was also found that the reaction efficiency and rate were greatly affected by the current intensity. For example, it took 70 hours to complete the reaction at a lower current intensity of 2.5 mA (entry 11 in Figure 1B). In contrast, a higher current intensity of 10 mA resulted in only a 13% yield of **8** (entry 12 in Figure 1B). The essentiality of $NiCl_2$·DME pre-catalyst, dtbbpy ligand, electrolysis, and supporting electrolyte was confirmed by control experiments (entries 1 – 5 in Figure 1B).

After optimizing the reaction conditions, we explored the substrate scope. As shown in Figure 2, OTs and OTf substituted 4-tert-butylbenzene are effective electrophiles, yielding 52% and 78% of product **8**, respectively. Other aryl bromides, including both electron-rich and electron-deficient arenes, were suitable electrophiles for this cross-coupling reaction (**9** to **19**). The aryl bromides with electron-rich substituents (**8** to **14**) delivered slightly higher yields (49% to 72%) compared to those with electron-deficient substituents (**15** to **19**, with yields ranging from 42% to 66%). This may be due to the low reactivity of electron-rich aryl bromides in the oxidative addition reaction with the Ni^I intermediate, which slows down the competing homo-coupling reaction of aryl bromides.[27] The aryl bromide electrophiles with various functional groups, including methoxy group (**11** and **12**), ester (**15**), fluoride (**16**), ketone (**18**), and trifluoromethyl group (**19**), as well as protection groups such as amide (**13**), acetal (**14**), and tert-butyloxycarbonyl (Boc) (**20** and **21**), were found to be effective in this reaction. The *para*-substituted methoxy bromobenzene delivered a yield comparable to that of the *meta*-substituted methoxy bromobenzene (52% yield for **11** and 49% yield for **12**). While the $C(sp^3)$–$C(sp^2)$ cross-coupling product was not obtained when using *ortho*-substituted methoxy bromobenzene electrophile. When the aryl halide contains F, Cl, and Br, the C–Br bond is selectively functionalized. Yields of 54% and 61% were obtained for products **16** and **17**, respectively, from 1-bromo-4-fluorobenzene and 1-bromo-4-chlorobenzene. For substrates with strong electron-withdrawing substituents such as methoxycarbonyl (**15**) and acetyl (**18**) groups, and π-conjugation extended aryl groups (**22**), the use of the 2,2'-bpy ligand resulted in the most favorable results (with yields of 66%, 42%, and 51% for **15**, **18**, and **22**, respectively). Aryl bromide electrophiles containing nitrogen-containing heterocyclic groups, such as Boc-protected tetrahydroisoquinoline and indole, also delivered yields of 61% (**20**) and 63% (**21**).

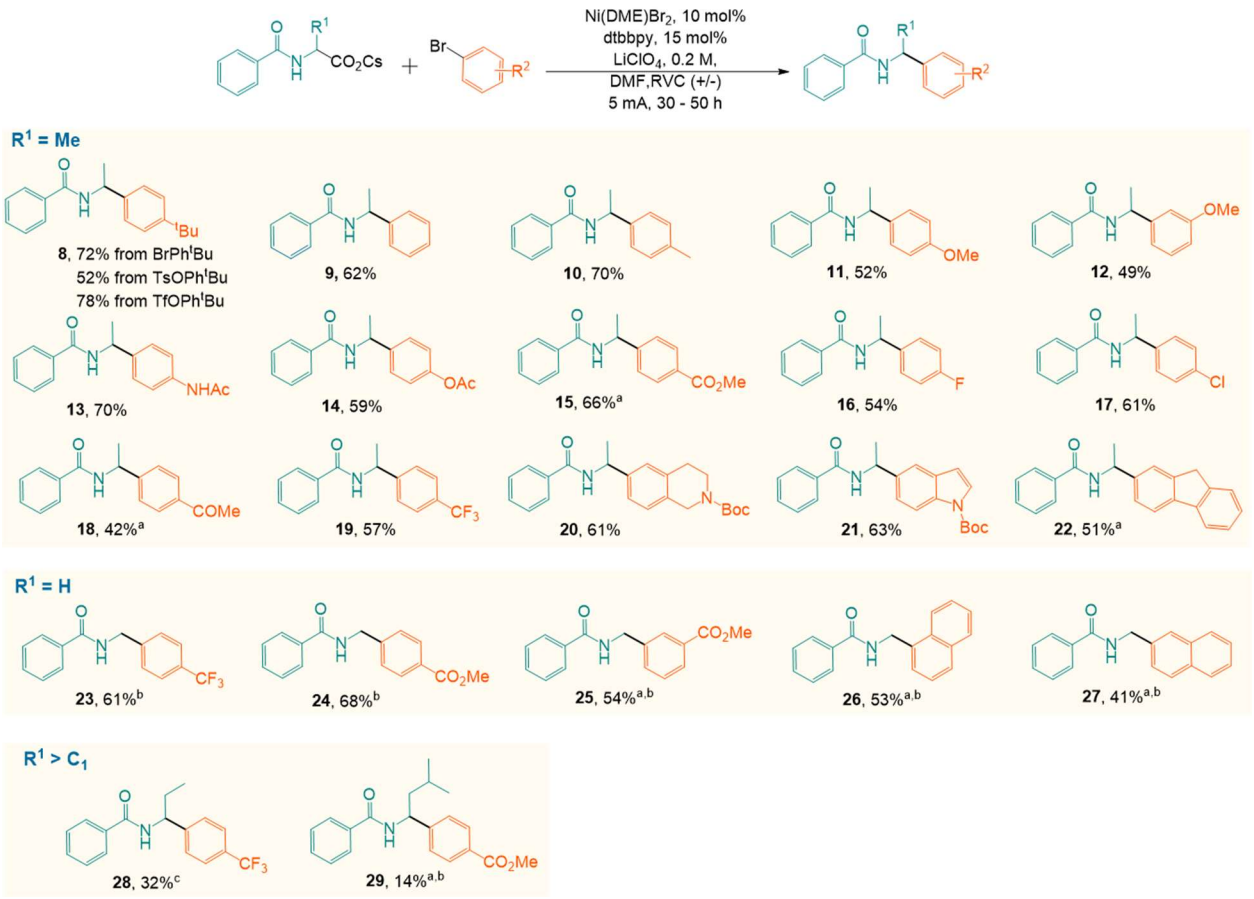

Figure 2. Reaction scope of the electro/Ni dual-catalyzed decarboxylative C(sp^3)–C(sp^2) cross-coupling reactions between α-amino acid and aryl bromide. Yields refer to yields of the isolated products after chromatography on silica gel. Reaction conditions: 0.65 mmol carboxylate, 0.5 mmol aryl bromide, 20 mg (0.075 mmol) dtbbpy ligand, 16 mg (0.05 mmol) $Ni(DME)Br_2$, 0.2 M $LiClO_4$ supporting electrolyte, 6 mL dry DMF, RVC (+/-), 5 mA current for 30 – 50 h. [a]2,2'-bpy as ligand, [b]$TBAPF_6$ as supporting electrolyte, [c]mixture of C(sp^3)–C(sp^2) cross-coupling product **28** and C(sp^2)–O cross-coupling product **28'**.

We also investigated the scope of carboxylate nucleophiles. Comparable yields were obtained when using N-benzoyl-glycine cesium salt as the precursor for the carbon radical. For instance, the yields of products **23** and **24** were 61% and 68%, respectively, which were comparable to the yields of products **19** and **15** (66% and 57%). The *para*-substituted bromobenzene delivered a slightly higher yield than the *meta*-substituted bromobenzene (68% yield for **24** and 54% yield for **25**). The π-conjugation extended aryl bromide substrates, 1-bromonaphthalene, and 2-bromonaphthalene, underwent this cross-coupling reaction smoothly, giving moderate yields of

53% and 41% for **21** and **22**, respectively. However, the yield of the decarboxylative C(sp^3)–C(sp^2) cross-coupling product dramatically decreased as the size of the group bonded to the α-carbon of the carboxyl group (-R_1) increased. Only 32% and 14% yields were obtained for **28** and **29**, respectively. Further increasing the size of the -R_1 group, no decarboxylative C(sp^3)–C(sp^2) cross-coupling product was obtained.

Other carboxylates shown in Figure 1A were also tested in the electro/Ni dual-catalyzed decarboxylative C(sp^3)–C(sp^2) cross-coupling reaction. As shown in Figure S2, the homo-coupling product, dimethyl 4,4'-biphenyldicarboxylate, was obtained as the main product for compounds **1**, **5**, and **6** in the reaction with methyl 4-bromobenzoate. In the case of compound **4**, the electrolysis cannot be processed as the cell voltage is high (> 6 V). Benzyl carboxylate **2** was found to be an efficient nucleophile in the decarboxylative C(sp^3)–C(sp^2) cross-coupling reaction with methyl 4-bromobenzoate. Product **30** was obtained with a yield of 58% in this study, which is significantly higher than the yield reported in our previous study using the combination of phenylacetic acid and Cs_2CO_3 (17% yield).[15] It is likely due to the low efficiency of *in situ* deprotonation of the phenylacetic acid/Cs_2CO_3 combination.

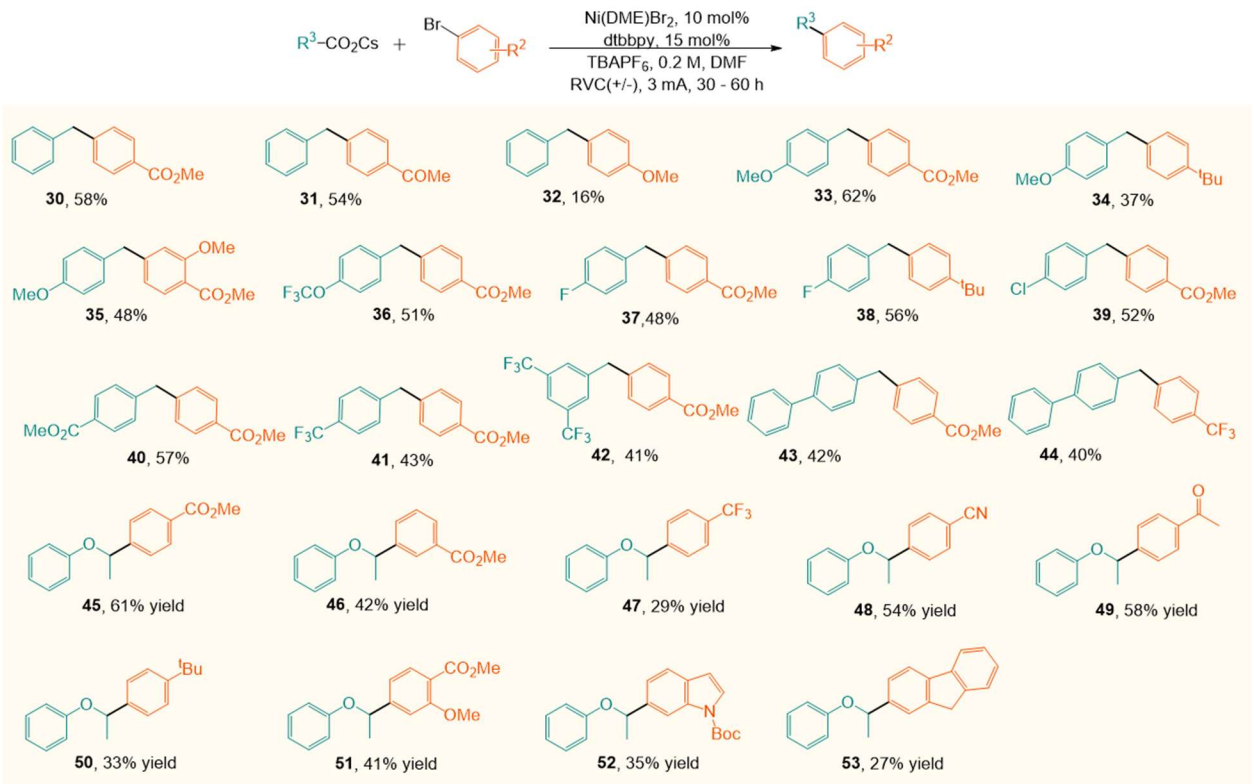

Figure 3. Reaction scope of the electro/Ni dual-catalyzed decarboxylative C(sp^3)–C(sp^2) cross-coupling reactions between aryl bromide and benzyl carboxylic acid or 2-phenoxy propionate. Yields refer to yields of the isolated products after chromatography on silica gel. Reaction conditions: 0.65 mmol carboxylate, 0.5 mmol aryl bromide, 20 mg (0.075 mmol) dtbbpy ligand, 16 mg (0.05 mmol) $NiBr_2$·DME, 0.2 M $TBAPF_6$ supporting electrolyte, 7.5 mL dry DMF, RVC (+/-), 3 mA current for 30 – 60 h.

As shown in Figure 3, the scope of benzyl carboxylate nucleophiles was also examined. Both electron-rich and electron-deficient benzyl carboxylates were efficient precursors in this cross-coupling reaction (**30** to **44**, up to 62 % yield for **33**). Various functional groups, such as the methoxy group (**32** and **35**), trifluoromethoxy group (**36**), ester (**30**, **33**, **35**, **36**, **37**, and **39** to **43**), ketone group (**31**), and trifluoromethyl group (**41**, **42**, and **44**), were found to be compatible with this reaction. The aryl bromides with electron-rich substituents (**32** and **34**, 16% and 37% yields) delivered lower yields than the ones with electron-deficient substituents (**30** and **33**, 58 % and 62% yields). Additionally, we noticed that the reaction yield decreased as the electron-withdrawing effect of the substituents on the benzyl carboxylate nucleophiles increased. For instance, when the substituent changed from the electron-donating methoxy (-OMe) group and hydrogen atom to the electron-withdrawing –Cl, –F, and $–CF_3$ groups, the yield decreased from 62% for **33** and 58% for **30** to 52% for **39**, 48% for **37**, and 43% for **41**. Electrochemical CV studies revealed that electron-withdrawing substituents reduced the electrochemical activity of the benzyl carboxylate (Figure S3A). The decrease in reaction yield is consistent with the positive shift in the onset oxidation potential of the benzyl carboxylates and the increase in the Hammett value of the substituents (Figure S3B). The π-conjugation extended 4-biphenylacetate is also reactive in this decarboxylative C(sp^3)–C(sp^2) cross-coupling reaction. Products **43** and **44** were obtained in 42% and 40% yields, respectively.

As mentioned above, the α-oxygen-substituted tetrahydrofuran-2-carboxylate **4** is not an efficient nucleophile for this decarboxylative C(sp^3)–C(sp^2) cross-coupling reaction (Figure S2). However, a linear 2-phenoxy propionate exhibited good reactivity and delivered a yield of 61% for the cross-coupling product **45** in reactions with aryl bromides. As shown in Figure 3, electron-rich, electron-deficient, and π-conjugation extended aryl bromides were all efficient substrates for this cross-coupling reaction, resulting in yields ranging from 27% to 61% for products **45** to **53**. Various functional groups, such as ester (**45**, **46**, and **51**), trifluoromethyl group (**47**), cyano group

(**48**), ketone group (**49**), methoxy group (**51**), and tert-butyloxycarbonyl (Boc) (**52**), were found to be compatible with 2-phenoxy propionate for electrosynthesis.

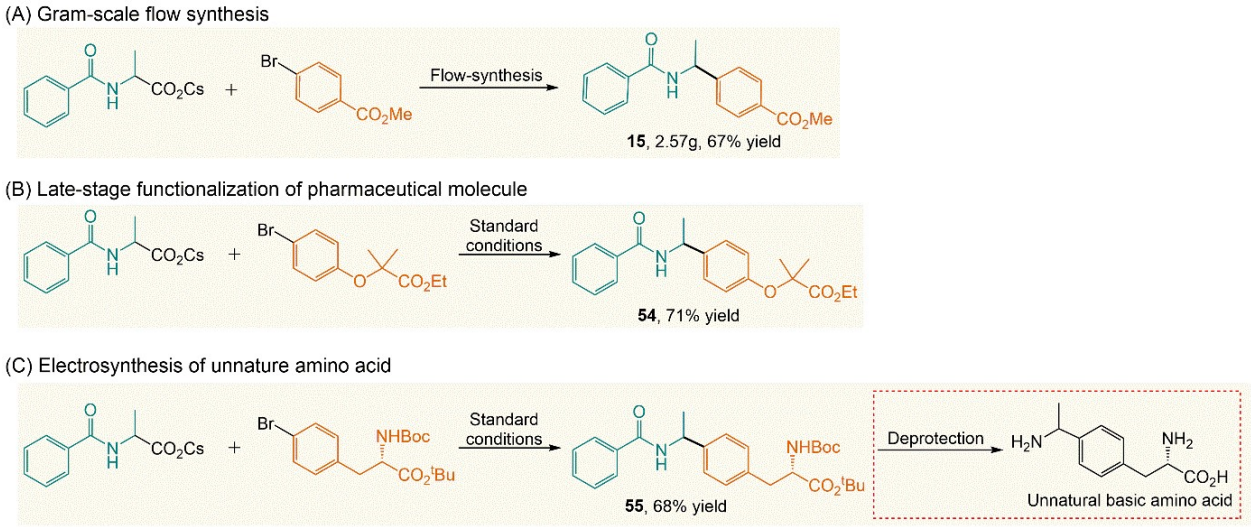

Figure 4. Gram-scale flow synthesis and applications of the electro/Ni dual-catalyzed decarboxylative C(sp^3)-C(sp^2) cross-coupling reaction. (A) Gram-scale flow-cell synthesis of product **15**, (B) Late-stage functionalization of Clofibrate, (C) Electrochemical synthesis of an unnatural amino acid. Yields refer to the isolated products after chromatography on silica gel.

To showcase the potential industrial adoption of the described electro/Ni dual-catalyzed C(sp^3)–C(sp^2) cross-coupling reactions, we performed a gram-scale synthesis of product **15** using a flow-cell reactor (Figure 4A). Under the flow-synthesis conditions, a yield of 67% was obtained for **15**, which is comparable to the yield obtained in the vial reaction (66%). To further demonstrate the potential applications of this methodology, we applied the decarboxylative C(sp^3)–C(sp^2) cross-coupling in the late-stage functionalization of pharmaceuticals. As shown in Figure 4B, a Clofibrate derivative was converted into a new compound, **54**, with a yield of 71%. In addition, this reaction was also effective in modifying natural amino acids. For example, a yield of 68% was obtained for compound **55** from the brominated phenylalanine (Figure 4C). After deprotecting compound **55**, a new synthetic unnatural basic amino acid can be produced.

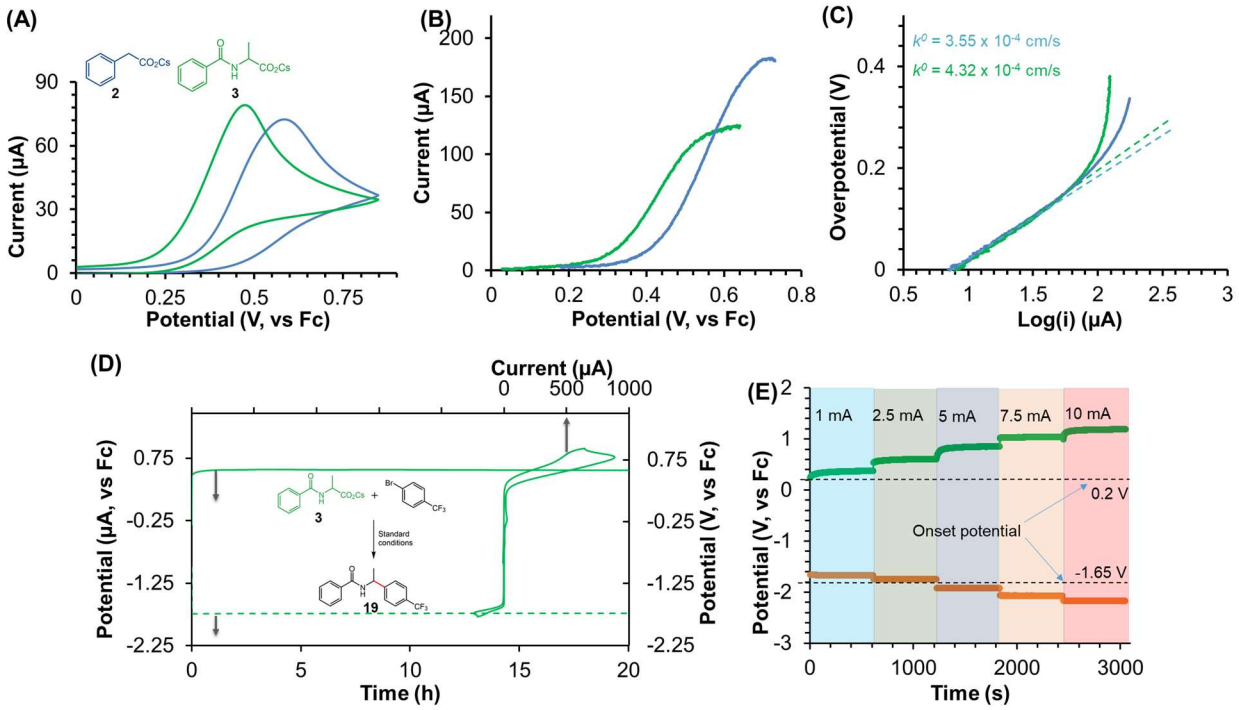

Figure 5. Electrochemical kinetics and reaction mechanism studies of the electro/Ni dual-catalyzed reaction system. (A) CV curves of carboxylates **2** and **3**; (B) RDE curves of carboxylates **2** and **3**; (C) Plots of overpotential versus the logarithm of kinetic current and the fitted Tafel plots of carboxylates **2** and **3**; (D) CV curve of the reaction mixture and monitored electrode potentials during the electrolysis; (E) Monitored electrode potentials during electrolysis under various operational current intensities.

In order to gain mechanistic insight into the cross-coupling transformation, we conducted electrochemical studies on carboxylates **2** and **3**. As shown in Figure 5A, compounds **2** and **3** exhibited onset oxidation potentials of 0.33 V and 0.26 V (vs. $Fc^{+/0}$), respectively. The RDE curves of compounds **2** and **3** were collected in DMF. The plots of overpotential versus the logarithm of kinetic current and the corresponding Tafel plots were constructed to determine the charge transfer rate constants (k^0) of the carboxylates in the anodic oxidation process (Figure 5B and 5C, refer to the SI for details).[26] The k^0 of the carboxylates was calculated as 3.55×10^{-4} cm/s for compound **2** and 4.32×10^{-4} cm/s for compound **3**, respectively. The higher k^0 of compound **3** indicates that the electrochemical oxidation process of compound **3** is faster than that of compound **2**. This is consistent with the slightly higher reaction efficiency of compound **3** compared to compound **2** in the cross-coupling reaction (Figures 2 and 3).

As shown in Figure 5D, the CV curve of the decarboxylative $C(sp^3)$–$C(sp^2)$ cross-coupling reaction mixture displayed a cathodic peak with an onset potential of -1.65 V (vs. $Fc^{+/0}$) for the reduction of the Ni^{II} catalyst and an anodic peak with an onset potential of 0.20 V (vs. $Fc^{+/0}$) for the oxidation of the carboxylate. The potentials of the cathode and anode were maintained at about -1.74 and 0.56 V (vs. $Fc^{+/0}$), respectively, during the electrolysis. The overpotentials for the cathodic and anodic half-reactions are 0.09 V and 0.36 V, respectively. As shown in Figure 5E, the overpotential of the anode increased more rapidly than that of the cathode as the operational current intensity increased. This indicates that the reaction kinetics of the cathodic half-reaction is faster than that of the anodic half-reaction.

In parallel with the experimental studies, we used DFT calculations to examine the details of the microscopic catalytic reaction steps that lead to both decarboxylation and $C(sp^3)$–$C(sp^2)$ cross-coupling. See the SI for complete computational modeling details. Figure 6 shows the potential-energy profile with enthalpy and Gibbs energies for the Ni-catalyzed cross-coupling between methyl 4-bromobenzoate and the carboxylates. This pathway involves the electrochemical one-electron reduction of pre-catalyst **A** [$Ni^{II}Br_2L$] to the active species **B** [$Ni^{I}BrL$] and loss of bromide. This provides a vacant coordination site at the Ni center to allow for slightly endergonic aryl bromide coordination and subsequent oxidative addition through **TS1**. This oxidative addition transition state requires a $\Delta G^{\ddagger}$ value of only 6.9 kcal/mol relative to **B**. The resulting five-coordinate [$ArNi^{III}Br_2L$] intermediate **D** is subsequently converted to [$LNi^{II}(Ar)Br$] species **E** through an exergonic electrochemical (by the cathode) or chemical (comproportionation with **B**) reduction step. The carbon free radical **H**, generated through oxidative decarboxylation of the carboxylates **F** at the anode side, coordinates to the Ni^{II}-center of **E**, resulting in a Ni^{III} intermediate **I**. This intermediate is nearly 25 kcal/mol exergonic relative to **B**, the aryl halide, and the carboxylate. Importantly, the high-valent intermediate **I** has a small energy barrier of 9.0 kcal/mol for reductive elimination to yield the $C(sp^3)$–$C(sp^2)$ cross-coupling product **J** and regenerate the catalyst **B**. This reductive elimination step is highly exergonic with an ΔG value of more than -30 kcal/mol. Based on this energy profile, reductive elimination of intermediate **I** is likely the rate-limiting step due to the higher barrier of **TS2** compared to all other reaction steps.

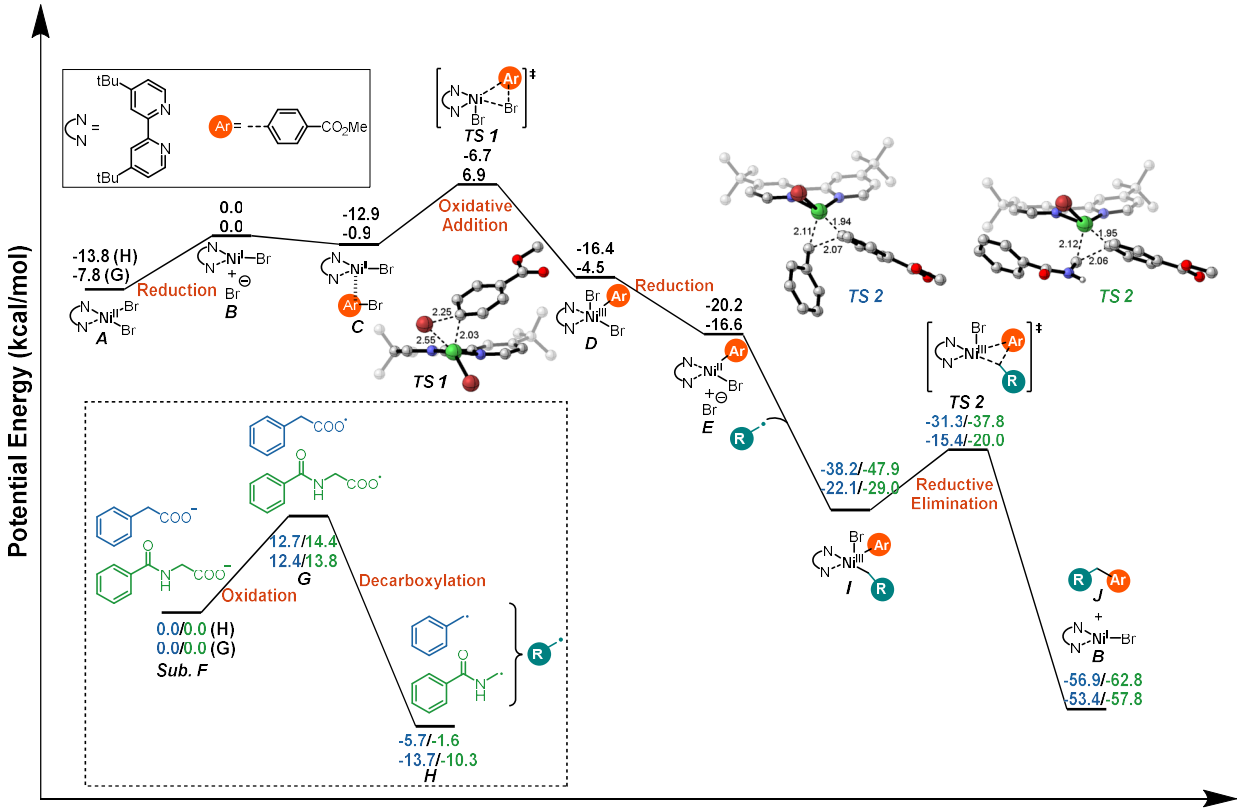

Figure 6. M06-L/6-31+G**(LANL2DZ) energy landscape for the Ni-catalyzed electrochemical decarboxylative C(sp^3)–C(sp^2) cross-coupling reaction between methyl 4-bromobenzoate and carboxylates.

While we explored several alternative reaction pathways that are detailed in the SI, it is useful to comment on the alternative pathway where the carboxylate-derived radical coordinates with the [Ni^{I}BrL] species **B** prior to the oxidative addition of the aryl bromide. As shown in Figure S6, on this energy profile, the carbon radical reacts directly with **B** to form [RNi^{II}BrL] species **C'**. While this is a favorable reaction step (ΔG = -11.9 kcal/mol), the subsequent single-electron reduction of **C'** to **D'** is significantly endergonic at 19.8 kcal/mol. This suggests that Ni^{II} species **C'** is more difficult to reduce at the cathode than other Ni^{II} (**A**, 7.8 kcal/mol) and Ni^{III} (**D**, -12.1 kcal/mol) species, and carbon radical is not included in the catalytic cycle until the [LNi^{II}(Ar)Br] species **E** is formed.

Conclusions

In summary, we report electro/Ni dual-catalyzed redox-neutral decarboxylative C(sp^3)–C(sp^2) cross-coupling reactions between carboxylates and aryl bromides. These reactions exhibit broad substrate scope, excellent functional-group tolerance, high selectivity, and good yields. The carboxylates, including amino acids, benzyl carboxylic acids, and 2-phenoxy propionic acid,

undergo oxidative decarboxylation at the anode to form carbon free radicals. The radicals then participate in the Ni-catalyzed cathodic C−Br activation reaction, resulting in the formation of $C(sp^3)$−$C(sp^2)$ cross-coupling products. The potential applications of this electrosynthesis method were demonstrated by gram-scale flow synthesis, late-stage functionalization of pharmaceuticals, and amino acid modification. The reaction mechanism was systematically studied through electrochemical voltammetry and DFT computational studies. The electro/Ni dual-catalyzed cross-coupling reactions described in this work are expected to have broad applications in the construction of $C(sp^3)$−$C(sp^2)$ bonds due to the readily availability of carboxylate nucleophiles and the scalability of electrochemical flow-synthesis technology.

Supporting Information

Supporting Information is available online or from the author. Experimental procedures, additional electrochemical, NMR analysis data, kinetic studies, the details of DFT calculation, and compound characterization data.

Acknowledgments

We thank the National Institutes of Health (grant no. R15GM143721) and the National Science Foundation (grant no. 1847674) for supporting this study. We acknowledge that the NMR studies are supported by NSF's MRI program (award number 1429195).

References:

(1) Tasker, S. Z.; Standley, E. A.; Jamison, T. F. *Nature* **2014**, *509*, 299.
(2) Diccianni, J. B.; Diao, T. *Trends Chem.* **2019**, *1*, 830.
(3) Ogoshi, S. *Nickel Catalysis in Organic Synthesis*; John Wiley & Sons: 2020.
(4) Montgomery, J. *Angew. Chem. Int. Ed.* **2004**, *43*, 3890.
(5) Fu, G. C. *ACS Central Sci.* **2017**, *3*, 692.
(6) Jana, R.; Pathak, T. P.; Sigman, M. S. *Chem. Rev.* **2011**, *111*, 1417.
(7) Han, F.-S. *Chem. Soc. Rev.* **2013**, *42*, 5270.
(8) Bhakta, S.; Ghosh, T. *Adv. Synth. Catal.* **2020**, *362*, 5257.
(9) Hazari, N.; Melvin, P. R.; Beromi, M. M. *Nat. Rev. Chem.* **2017**, *1*, 0025.
(10) Yan, M.; Kawamata, Y.; Baran, P. S. *Chem. Rev.* **2017**, *117*, 13230.
(11) Zhang, S.; Findlater, M. *Chem. Eur. J.* **2022**, *28*, e202201152.
(12) Novaes, L. F. T.; Liu, J.; Shen, Y.; Lu, L.; Meinhardt, J. M.; Lin, S. *Chem. Soc. Rev.* **2021**, *50*, 7941.
(13) Tay, N. E. S.; Lehnherr, D.; Rovis, T. *Chem. Rev.* **2022**, *122*, 2487.
(14) Zhang, L.; Hu, X. *Chem. Sci.* **2020**, *11*, 10786.
(15) Luo, J.; Hu, B.; Wu, W.; Hu, M.; Liu, T. L. *Angew. Chem. Int. Ed.* **2021**, *60*, 6107.
(16) Moon, P. J.; Lundgren, R. J. *ACS Catal.* **2020**, *10*, 1742.

(17) Shang, R.; Liu, L. *Sci. China Chem.* **2011**, *54*, 1670.
(18) Ramadoss, V.; Zheng, Y.; Shao, X.; Tian, L.; Wang, Y. *Chem. Eur. J.* **2021**, *27*, 3213.
(19) Shi, S.-H.; Liang, Y.; Jiao, N. *Chem. Rev.* **2021**, *121*, 485.
(20) Leech, M. C.; Lam, K. *Acc. Chem. Res.* **2020**, *53*, 121.
(21) Kolbe, H. *J. Prakt. Chem.* **1847**, *41*, 137.
(22) Hioki, Y.; Costantini, M.; Griffin, J.; Harper, K. C.; Merini, M. P.; Nissl, B.; Kawamata, Y.; Baran, P. S. *Science* **2023**, *380*, 81.
(23) Mo, Y.; Lu, Z.; Rughoobur, G.; Patil, P.; Gershenfeld, N.; Akinwande, A. I.; Buchwald, S. L.; Jensen, K. F. *Science* **2020**, *368*, 1352.
(24) Harwood, S. J.; Palkowitz, M. D.; Gannett, C. N.; Perez, P.; Yao, Z.; Sun, L.; Abruña, H. D.; Anderson, S. L.; Baran, P. S. *Science* **2022**, *375*, 745.
(25) Palkowitz, M. D.; Laudadio, G.; Kolb, S.; Choi, J.; Oderinde, M. S.; Ewing, T. E.-H.; Bolduc, P. N.; Chen, T.; Zhang, H.; Cheng, P. T. W.; Zhang, B.; Mandler, M. D.; Blasczak, V. D.; Richter, J. M.; Collins, M. R.; Schioldager, R. L.; Bravo, M.; Dhar, T. G. M.; Vokits, B.; Zhu, Y.; Echeverria, P.-G.; Poss, M. A.; Shaw, S. A.; Clementson, S.; Petersen, N. N.; Mykhailiuk, P. K.; Baran, P. S. *J. Am. Chem. Soc.* **2022**, *144*, 17709.
(26) Bard, A. J.; Faulkner, L. R.; White, H. S. *Electrochemical methods: fundamentals and applications*; John Wiley & Sons, 2022.
(27) Luo, J.; Davenport, M. T.; Carter, A.; Ess, D. H.; Liu, T. L. *Faraday Discuss.* **2023**, doi.org/10.1039/D3FD00069A.